First Principles Study on the Magnetism of Rectangular Nanosilicenes *

Rui-Kuan Xie(解瑞宽)[1], Ai-Jiang Lu(陆爱江)[1], Huai-Zhong Xing(邢怀中)[1**], Yi-Jie Zeng(曾宜杰)[1], Yan Huang(黄燕)[2**], Xiao-Shuang Chen(陈效双)[2]

[1]*Department of Applied Physics and State Key Laboratory for Modification of Chemical Fibers and Polymer Materials, Donghua University, Shanghai 201620*

[2]*National Lab of Infrared Physics, Shanghai Institute for Technical Physics, Chinese Academy of Sciences, Shanghai 200083*

(Received 18 August 2017)

We present first-principle calculations on the magnetism in finite rectangular nanosilicenes (RNSs). An antiferromagnetic (AFM) state at two zigzag edges is found when the RNSs approach a critical size. This AFM state originates from the localized p_z orbits of Si atoms at the edges, similar to those in the infinitely long zigzag-edged silicon nanoribbons. The smallest RNS that can maintain the AFM phase as the ground state is identified. It is also found that aluminum dopants can regulate the distribution of the spin density and the energy difference between AFM and FM states.

PACS: 73.22.−f, 75.25.−j DOI: 10.1088/0256-307X/35/1/017301

Graphene, a two-dimensional honeycomb network of carbon atoms, has attracted a great deal of interest because of its unique electronic properties and potential applications in future nanoelectronic devices.[1−4] The outstanding success in the investigations of graphene has motivated scientists to study its hypothetical silicon counterpart named as 'silicene' (a monolayer silicon sheet arranged in a honeycomb lattice).[5−8]

Recently, the growth of silicene on different substrates such as Ag (110), Ag (100), Ir(111) and ZrC (111) has been reported.[9−12] Also, theoretical studies have shown that silicene has basically the same electronic structure as graphene, such as gaplessness and linear energy–momentum relationship in the vicinity of the Dirac point.[13−16] Many expectations of graphene could be desired in silicene with the crucial advantage of easily matching into the silicon-based electronics industry. Differing from the flat graphene, silicene has a buckled honeycomb structure. This buckled structure produces an intrinsic Rashba spin–orbit coupling which plays an important role in spin transport.[17]

As quasi-1 nanomaterials for the nanoscience and nanotechnology, grapene nanoribbons have attracted much interest recently.[18−22] Silicon nanoribbons (SiNRs) are one method to open a band gap and have been grown on Au (110) and Ag(110) with both zigzag edge (ZSiNRs) and armchair edge (ASiNRs).[23−25] Meanwhile, the electronic band structures and magnetic properties of SiNRs have been studied by theoretical works. A spin state appears at the two zigzag edges which originates from the localized p_z orbits at the edge sides. Ding and Ni found an AFM ground state, where spin-up electrons and spin-down electrons were separated on the two edges in ZSiNRs.[26] The electronic and magnetic properties of Si materials doped with boron (B), nitrogen (N) and Al atoms have been studied.[27−31] It was found that these dopants can greatly affect the band structure of the ribbons and can turn the edges into nonmagnetic (NM) phase.[28,29]

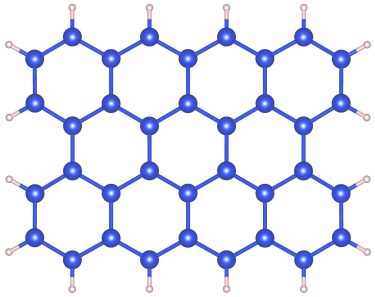


Fig. 1. Atomic structure of RNS [4,3]. Silicon atoms are shown in blue and H atoms in white. There are 4 rings along the zigzag edge and 3 rings along the armchair edge.

Because of the weak overlap between the $3p_z$ orbits of neighboring Si atoms the silicene surface becomes very reactive and can easily adsorb foreign chemical species.[32] However, in this study, we mainly focus our investigation on edge effects of π electrons on magnetism of nanosilicene. The dangling bonds of Si atoms on the edges were saturated by hydrogen atoms. We built the models of RNS $[X, Y]$, where X and Y represent the number of rings along the zigzag and armchair edges, respectively. For example, the atomic structure of RNS [4,3] is shown in Fig. 1.

The calculations are based on density functional theory (DFT) using the plane wave method encoded in the software Vienna ab initio simulation package (VASP).[33] We use the generalized gradient approximation (GGA) of Perdew–Burke–Ernzerhof (PBE) functional for the exchange correlation potential.[34]

*Supported by the National Natural Science Foundation of China under Grant Nos 61376102 and 11174048, and the Computational Support from Shanghai Supercomputer Center.

**Corresponding author. Email: xinghz@dhu.edu.cn; yhuang@mail.sitp.ac.cn

© 2018 Chinese Physical Society and IOP Publishing Ltd

The electron wave function is expanded in plane waves and a cutoff energy of 500 eV is chosen. Only the Γ point is used to sample the Brillouin zone. The convergence in energy and force are set as 10^{-4} eV and 0.025 eV/Å.

Table 1. Energy difference between AFM, FM and NM phases of RNSs.

RNS $[X,Y]$	[3,3]	[3,5]	[3,7]	[3,9]	[4,3]	[5,3]	[5,5]	[7,5]	[9,5]
$E_{\rm FM}-E_{\rm NM}$ (meV)	0	0	−48	−70	−5	−97	−106	−96	−197
$E_{\rm AFM}-E_{\rm NM}$ (meV)	0	−13	−55	−73	−40	−106	−113	−146	−217

Table 1 lists the energy differences of three magnetic phases (AFM, FM and NM) of RNSs with different sizes. From Table 1 we can see that RNS [3,3] has no magnetic phase (both AFM and FM phases converged to the NM phase). It is common in the RNSs smaller than RNS [3,3], thus they are not listed in this table. Notice that RNS [3,5] does not have the FM phase and the energy difference between AFM and NM phases is as small as 13 meV. For RNS [4,3], the AFM and FM phases are more stable than the NM phase, whereas their energy is pretty close. For other RNSs with longer zigzag and armchair edges than RNS [3,3], the FM phase is energetically between the AFM and NM phase while the AFM phase is the most favorable one. The above information indicates that RNSs [3,5] and [4,3] are the transition structures between a nonmagnetic RNS [3,3] and larger RNSs that have more stable AFM phases and metastable FM phases. That is to say, for large RNSs, the stability trend is the same as what an infinitely long ribbon has, i.e., NM<FM<AFM. To investigate how RNS $[X,Y]$ approaches infinitely long zigzag ribbons in the stability respect, we compare the energy difference (normalized to the length X) between AFM and NM phases of rectangular RNSs with the infinitely long ribbon that has the same width (Y). Figure 2 shows that the above energy difference enhances much from RNS [3,5] to RNS [5,5]. The change from RNS [5,5] to [9,5] is much smaller. In general, the energy difference enlarges with the increase of X. It is worth noting that the change from RNS [9,5] to infinite ribbon is so small that we can obtain that for the RNSs between RNS [9,5] and infinite ribbon the vibration of the change can be ignored.

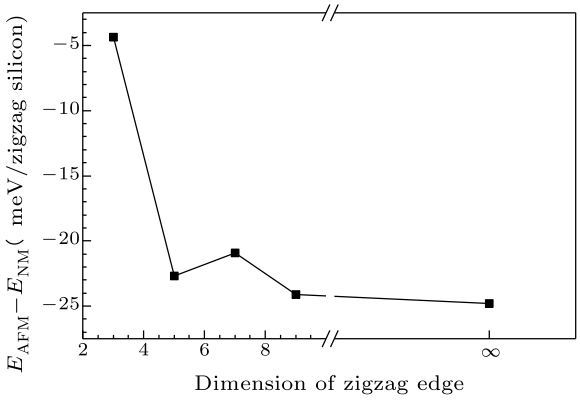


Fig. 2. Change of normalized energetic difference between the AFM and NM phases of RNS [X,5] with the dimension of the zigzag edge, X. The corresponding value for an infinitely long ribbon is also plotted.

Figure 3 shows the isosurfaces of spin density of the AFM and FM phases of RNS [5,5]. As presented in Figs. 3(a) and 3(b), in both AFM and FM phases, the magnetization mainly localizes at the zigzag edges. The closer the Si atom to the center of the zigzag edge is, the larger magnetic moment it has. In the FM phase, the spin directions at the two zigzag edges are the same. However, in the AFM phase they are opposite. There is small magnetization at the armchair edges which does not extend to the middle of these two edges.

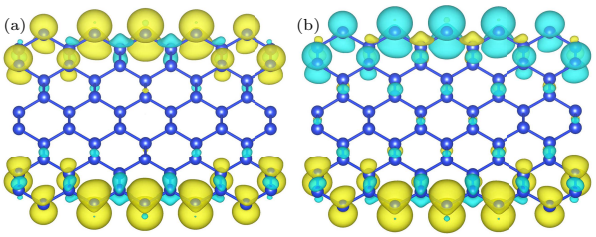


Fig. 3. Isosurfaces of spin density of the FM (a) and AFM (b) phases of RNS [5,5]. Yellow indicates spin-up density and blue indicates spin-down density, respectively. Here H atoms are not shown, and isosurface levels are set as 0.0038 Å^{-3}.

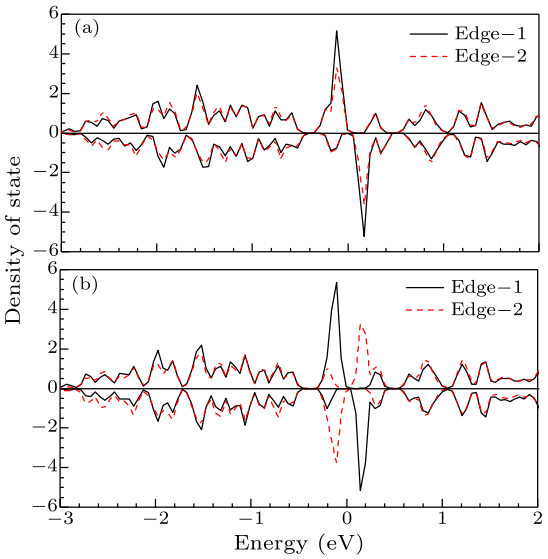


Fig. 4. Summation of the p_z-DOS of Si atoms at zigzag edges of RNS[5,5] in (a) FM phase and (b) AFM phase.

To investigate the origin of the spin states in RNSs, we calculate the summation of the p_z orbits at the two zigzag edges of RNS [5,5], as shown in Fig. 4. In the FM phase, the p_z orbits of the two edges have the same spin states and spin orientations near the Fermi level,

as shown in Fig. 4(a). In Fig. 4(b), for the AFM phase, the p_z orbits of the two edges are still the same but the spin orientations are opposite. The above information indicates that magnetization in RNSs originates from the localized p_z orbits at the zigzag edge sides as in the infinitely long zigzag ribbon of the same width.

Table 2 lists more information about different sizes of RNSs. In Table 2, for the AFM phase of RNS [X,5], the total spin-up magnetic moment is in direct proportion to the length of the zigzag edge just as the stability of the AFM phase listed in Table 1. However, for the FM phase of RNS [X,5], both the value of the total and the total spin-up magnetic moments take a jump from RNS [7,5] to RNS [9,5]. The total magnetic moment jumps from 2.5 to 4, while the value of the total spin-up magnetic moment jumps from 2.7 to 4.26. The average magnetic moments of the zigzag edge Si atoms are determined to be 0.164 μ_B, 0.178 μ_B, and 0.186 μ_B for RNSs [5,5], [7,5], and [9,5], respectively, approaching that of an infinitely long zigzag-edged ribbon with the same width (0.214 μ_B).

Table 2. Total magnetic moments and total spin-up moments for the FM phase ($M_{\mathrm{total-FM}}$ and $M_{\mathrm{up-FM}}$), total spin-up moments for the AFM phase ($M_{\mathrm{up-AFM}}$) and the averaged magnetic moment of the edge silicon atoms for AFM phases ($M_{\mathrm{AVG-AFM}}$).

Size	[3,3]	[3,5]	[3,7]	[3,9]	[4,3]	[5,3]	[5,5]	[7,5]	[9,5]
$M_{\mathrm{total-FM}}$ (μ_B)	0	0	2	2	2	2	2	2.5	4
$M_{\mathrm{up-FM}}$ (μ_B)	0	0	2.056	2.133	1.983	2.052	2.166	2.701	4.256
$M_{\mathrm{edge-FM}}$ (μ_B)	0	0	0.239	0.239	0.231	0.256	0.257	0.225	0.24
$M_{\mathrm{AVG-AFM}}$ (μ_B)	0	0.126	0.159	0.163	0.142	0.164	0.164	0.178	0.186
$M_{\mathrm{up-AFM}}$ (μ_B)	0	0.883	1.122	1.164	1.043	1.237	1.32	2.049	2.639

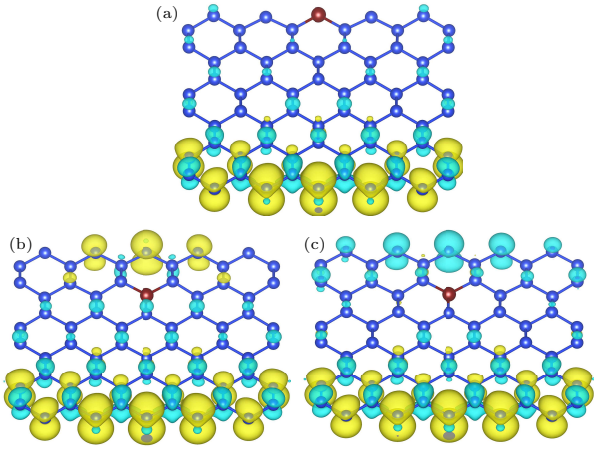


Fig. 5. Isosurfaces of spin density of the Al doped (a) on the edge of the RNS [5,5], (b) and (c) inside the RNS [5,5]. Yellow indicates spin-up density and blue indicates spin-down density, respectively. Al atoms are shown in brown. Here H atoms are not shown, and isosurface levels are set as 0.0038 Å^{-3}.

The effect of Al dopants on the magnetic distribution is investigated. One Al atom is doped into RNS [5,5] as presented in Fig. 5. The symmetric spin distribution is broken when the impurity is on the edge, see Fig. 5(a). The edge that doped with Al atom does not show any spin polarization. This is because the hole induced by the Al atom prefers to inject into edge π states, thus the spin polarization at the edge is compressed.[29] When the impurity is away from the edge, the RNS [5,5] can basically maintain the symmetry of the spin distribution as indicated in Figs. 5(b) and 5(c). In addition, we have also found that the energy difference between AFM and FM states is negligible in this case (about 1 meV), which is much less than the structure without Al dopants. Thus this is also a new way to regulate the stabilization and the distribution of the magnetic states of RNSs.

In summary, we have investigated magnetism in rectangular silicenes by first principles. It is found that when the RNS reaches the size of [4,3], an AFM phase appears at the two zigzag edges. This AFM phase arises from the localized p_z orbits at the zigzag edges just like that in the infinitely long zigzag-edges silicene nanoribbons. RNS [4,3] is found to be the smallest RNS that can maintain the AFM phase as the ground state. For larger RNSs with increased length of the zigzag edge and the same width, the stability of the AFM, FM and NM phases, the normalized energy difference between AFM and NM phases, and the average magnetic moment of Si atoms at zigzag edges are found to approach the infinitely long zigzag-edged ribbon with the same width. Lastly, we have also discussed the role of Al atoms in affecting the distribution of the spin polarization and pointed out that this is a new way of regulating the stabilization the magnetic states of RNSs. These RNSs are good candidates to verify the predicted characteristics of finitely long ribbons experimentally.

References

[1] Novoselov K S, Geim A K, Morozov S V, Jiang D, Zhang Y, Dubonos S V, Grigorieva I V and Firsov A A 2004 *Science* **306** 666
[2] Novoselov K S, Geim A K, Morozov S V, Jiang D, Katsnelson M I, Grigorieva I V, Dubonos S V and Firsov A A 2005 *Nature* **438** 197
[3] Castro Neto A H, Guinea F, Peres N M R, Novoselov K S and Geim A K 2009 *Rev. Mod. Phys.* **81** 109
[4] Geim A K and Novoselov K S 2007 *Nat. Mater.* **6** 183
[5] Kara A, Enriquez H, Seitsonen A P, Lew Yan Voon L C, Vizzini S, Aufray B and Oughaddou H 2012 *Surf. Sci. Rep.* **67** 1
[6] Butler S Z, Hollen S M, Cao L, Cui Y, Gupta J A, Gutiérrez H R, Heinz T F, Hong S S, Huang J, Ismach A F, Johnston-Halperin E, Kuno M, Plashnitsa V V, Robinson R D, Ruoff R S, Salahuddin S, Shan J, Shi L, Spencer M G, Terrones M, Windl W and Goldberger J E 2013 *ACS Nano* **7** 2898
[7] Xu M S, Liang T, Shi M M and Chen H Z 2013 *Chem. Rev.* **113** 3766
[8] Tao L, Cinquanta E, Chiappe D, Grazianetti C, Fanciulli M, Dubey M, Molle A and Akinwande D 2015 *Nat. Nanotechnol.* **10** 227

[9] Léandri C, Oughaddou H, Aufray B, Gay J M, Le Lay G, Ranguis A and Garreau Y 2007 *Surf. Sci.* **601** 262
[10] Kara A, Léandri C, Dávila M E, De Padova P, Ealet B, Oughaddou H, Aufray B and Le Lay G 2009 *J. Supercond. Novel Magn.* **22** 259
[11] Meng L, Wang Y L, Zhang L Z, Du S X, Wu R T, Li L F, Zhang Y, Li G, Zhou H T, Hofer W A and Gao H J 2013 *Nano Lett.* **13** 685
[12] Aizawa T, Suehara S and Otani S 2014 *J. Phys. Chem. C* **118** 23049
[13] Lebègue S and Eriksson O 2009 *Phys. Rev.* B **79** 115409
[14] Cahangirov S, Topsakal M, Aktürk E, Şahin H and Ciraci S 2009 *Phys. Rev. Lett.* **102** 236804
[15] Giovannetti G, Khomyakov P A, Brocks G, Kelly P J and van den Brink J 2007 *Phys. Rev.* B **76** 073103
[16] Chen L, Liu C C, Feng B, He X, Cheng P, Ding Z, Meng S, Yao Y and Wu K 2012 *Phys. Rev. Lett.* **109** 056804
[17] DyrdałA and Barnaś J 2012 *Phys. Status Solidi RRL* **6** 340
[18] Li X L, Wang X R, Zhang L, Lee S and Dai H J 2008 *Science* **319** 1229
[19] Han M Y, Özyilmaz B, Zhang Y and Kim P 2007 *Phys. Rev. Lett.* **98** 206805
[20] Jiao L Y, Zhang L, Wang X R, Diankov G and Dai H J 2009 *Nature* **458** 877
[21] Ruffieux P, Wang S, Yang B, Sánchez-Sánchez C, Liu J, Dienel T, Talirz L, Shinde P, Pignedoli C A, Passerone D, Dumslaff T, Feng X, Müllen K and Fasel R 2016 *Nature* **531** 489
[22] Magda G Z, Jin X, Hagymási I, Vancsó P, Osváth Z, Nemes-Incze P, Hwang C, Biró L P and Tapasztó L 2014 *Nature* **514** 608
[23] Rachid Tchalala M, Enriquez H, Mayne A J, Kara A, Roth S, Silly M G, Bendounan A, Sirotti F, Greber T, Aufray B, Dujardin G, Ait Ali M and Oughaddou H 2013 *Appl. Phys. Lett.* **102** 083107
[24] De Padova P, Kubo O, Olivieri B, Quaresima C, Nakayama T, Aono M and Le Lay G 2012 *Nano Lett.* **12** 5500
[25] De Padova P, Quaresima C, Ottaviani C, Sheverdyaeva P M, Moras P, Carbone C, Topwal D, Olivieri B, Kara A, Oughaddou H, Aufray B and Le Lay G 2010 *Appl. Phys. Lett.* **96** 261905
[26] Ding Y and Ni J 2009 *Appl. Phys. Lett.* **95** 083115
[27] Zberecki K, Swirkowicz R and Barnaś J 2014 *Phys. Rev.* B **89** 165419
[28] Fang D Q, Zhang S L and Xu H 2013 *RSC Adv.* **3** 24075
[29] Zheng F B, Zhang C W, Yan S S and Li F 2013 *J. Mater. Chem. C* **1** 2735
[30] Zhang J M, Song W T, Xu K W and Ji V 2014 *Comput. Mater. Sci.* **95** 429
[31] Chen A B, Wang X F, Vasilopoulos P, Zhai M X and Liu Y S 2014 *Phys. Chem. Chem. Phys.* **16** 5113
[32] Houssa M, Pourtois G, Afanas'ev V V and Stesmans A 2010 *Appl. Phys. Lett.* **97** 112106
[33] Kresse G and Furthmüller J 1996 *Phys. Rev.* B **54** 11169
[34] Perdew J P, Burke K and Ernzerhof M 1996 *Phys. Rev. Lett.* **77** 3865